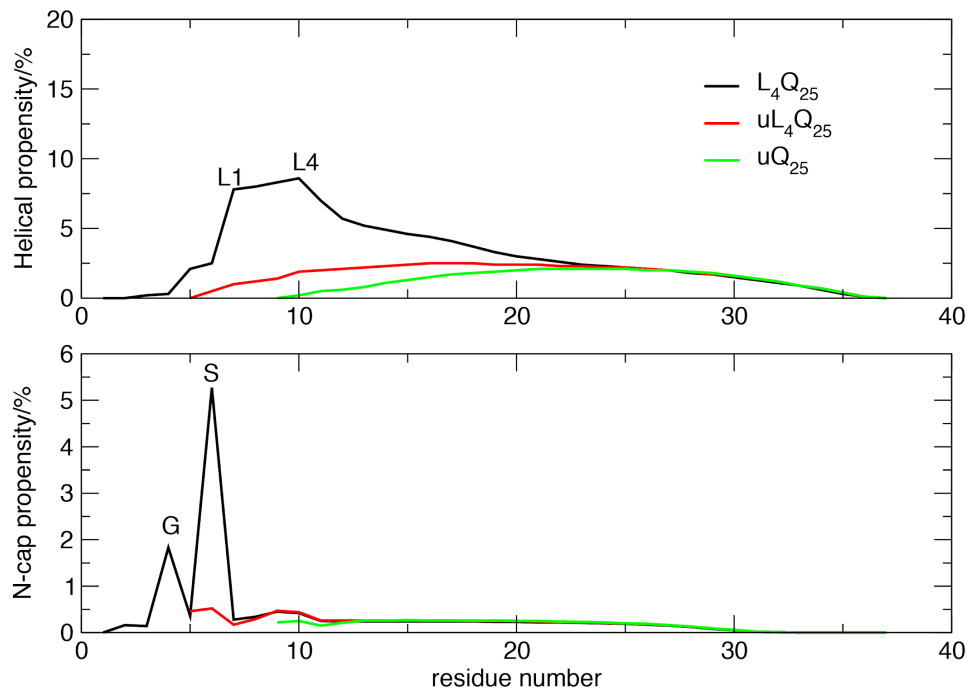
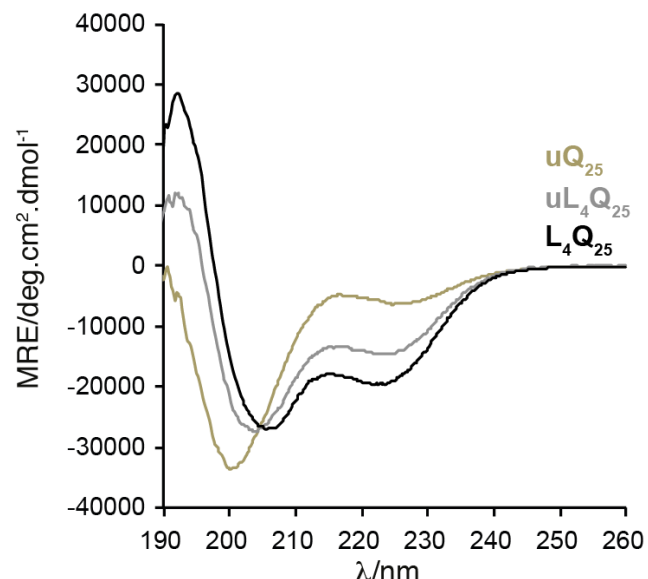


Side chain to main chain hydrogen bonds stabilize a polyglutamine helix in a transcription factor

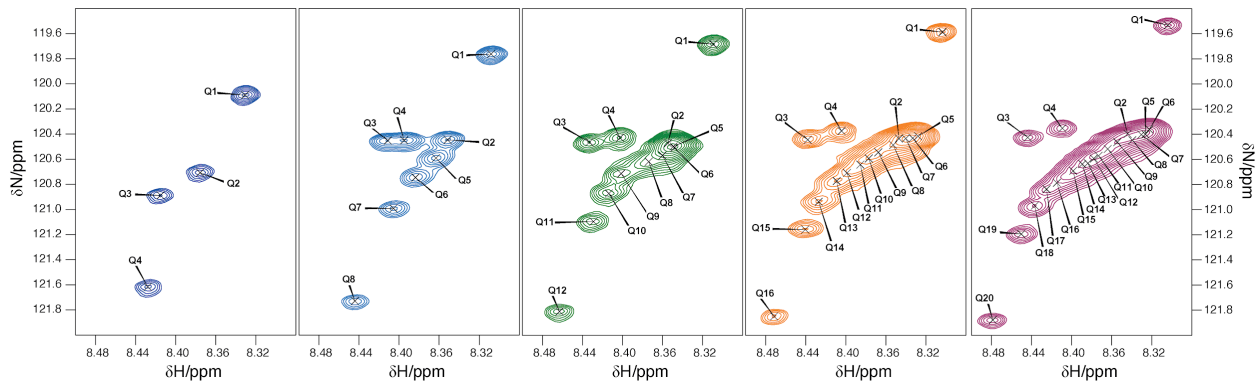
A. Escobedo, B. Topal et al.



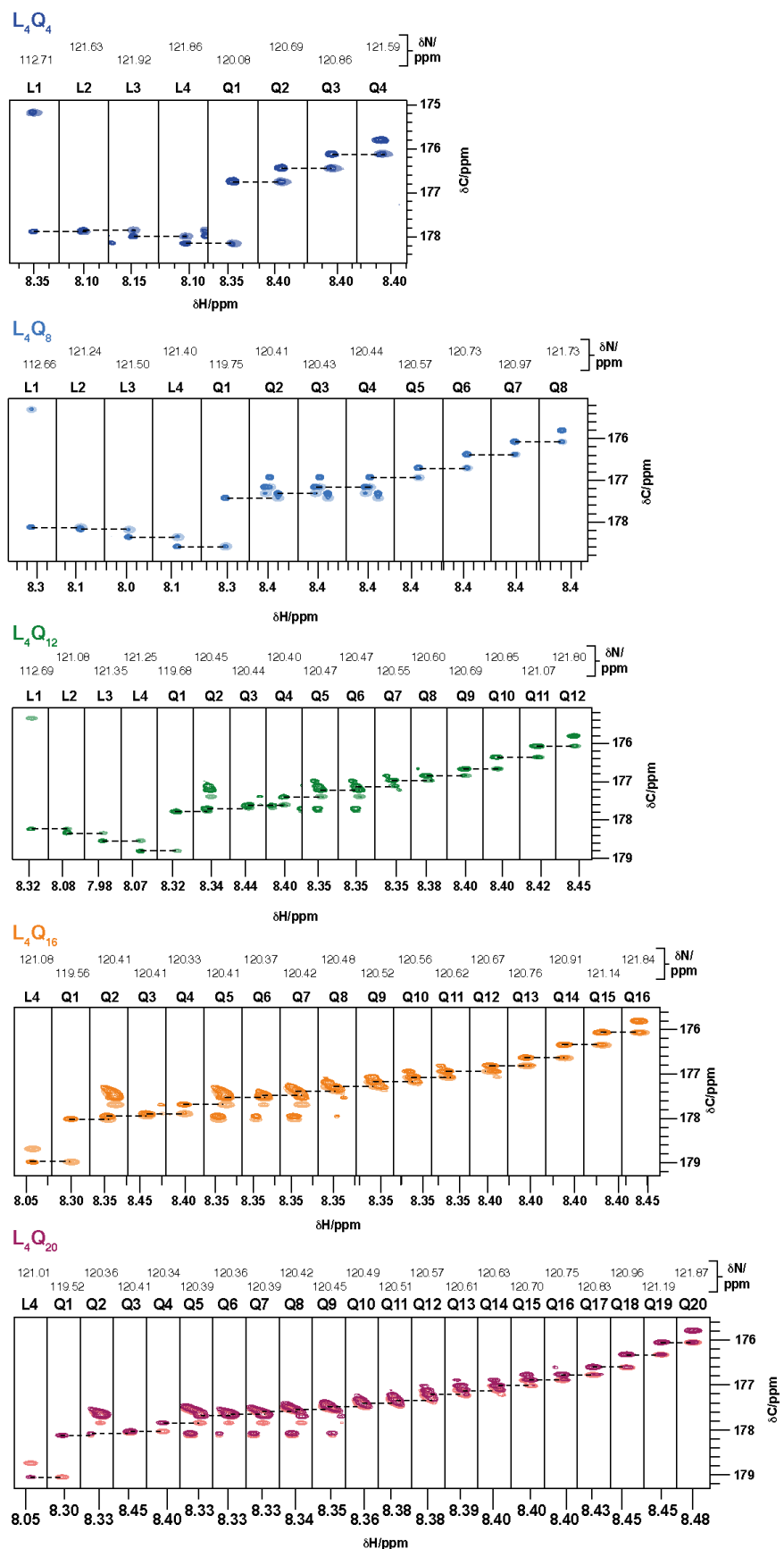
Supplementary Figure 1 | Prediction of helical and N-cap propensity, for peptides uQ_{25} , uL_4Q_{25} and L_4Q_{25} obtained by using Agadir¹. The peptides have been aligned so that the Gln residues, that are common to all of them, have the same residue numbers (Q11-Q35).



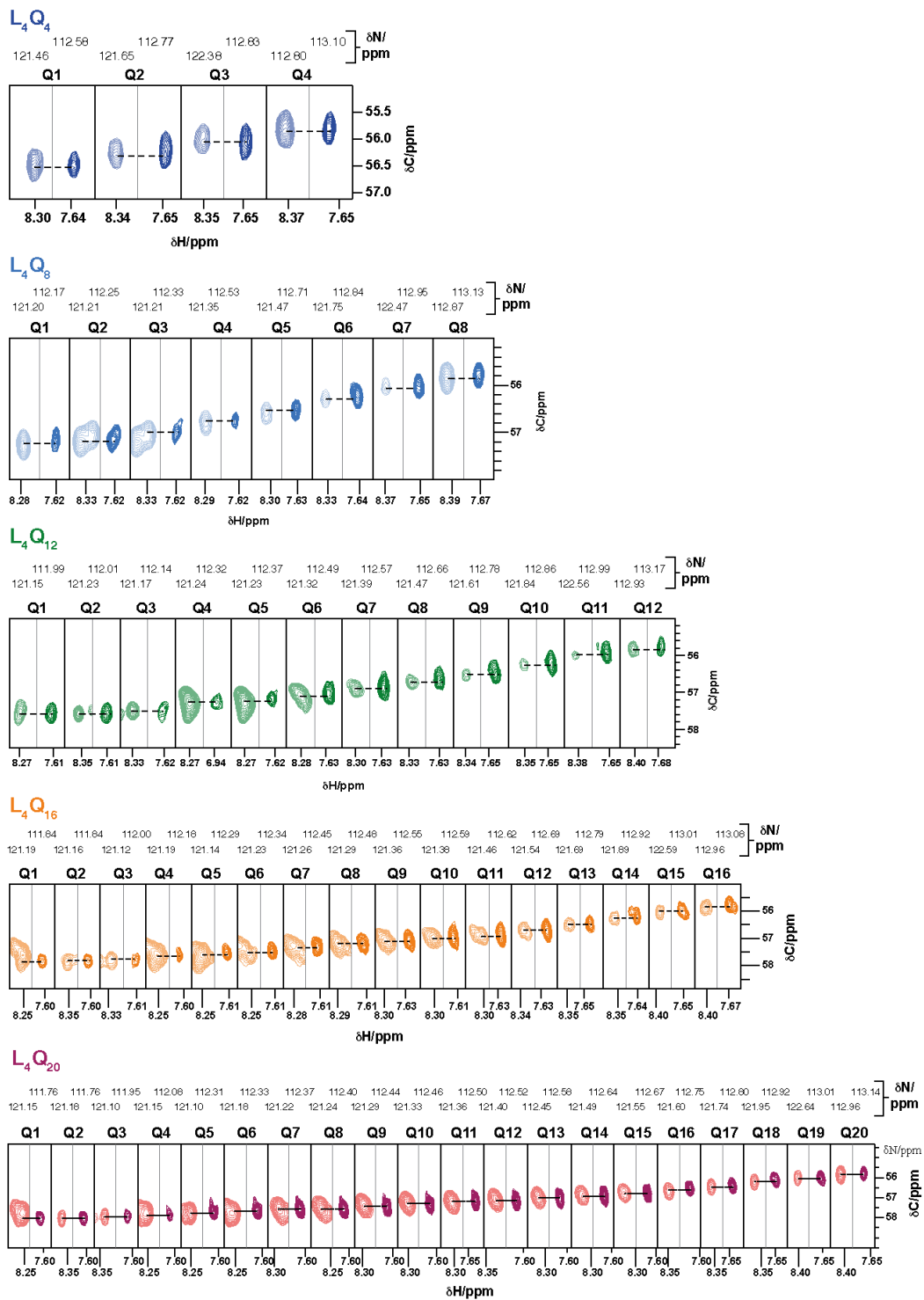
Supplementary Figure 2 | CD spectra of uQ_{25} , uL_4Q_{25} and L_4Q_{25} .



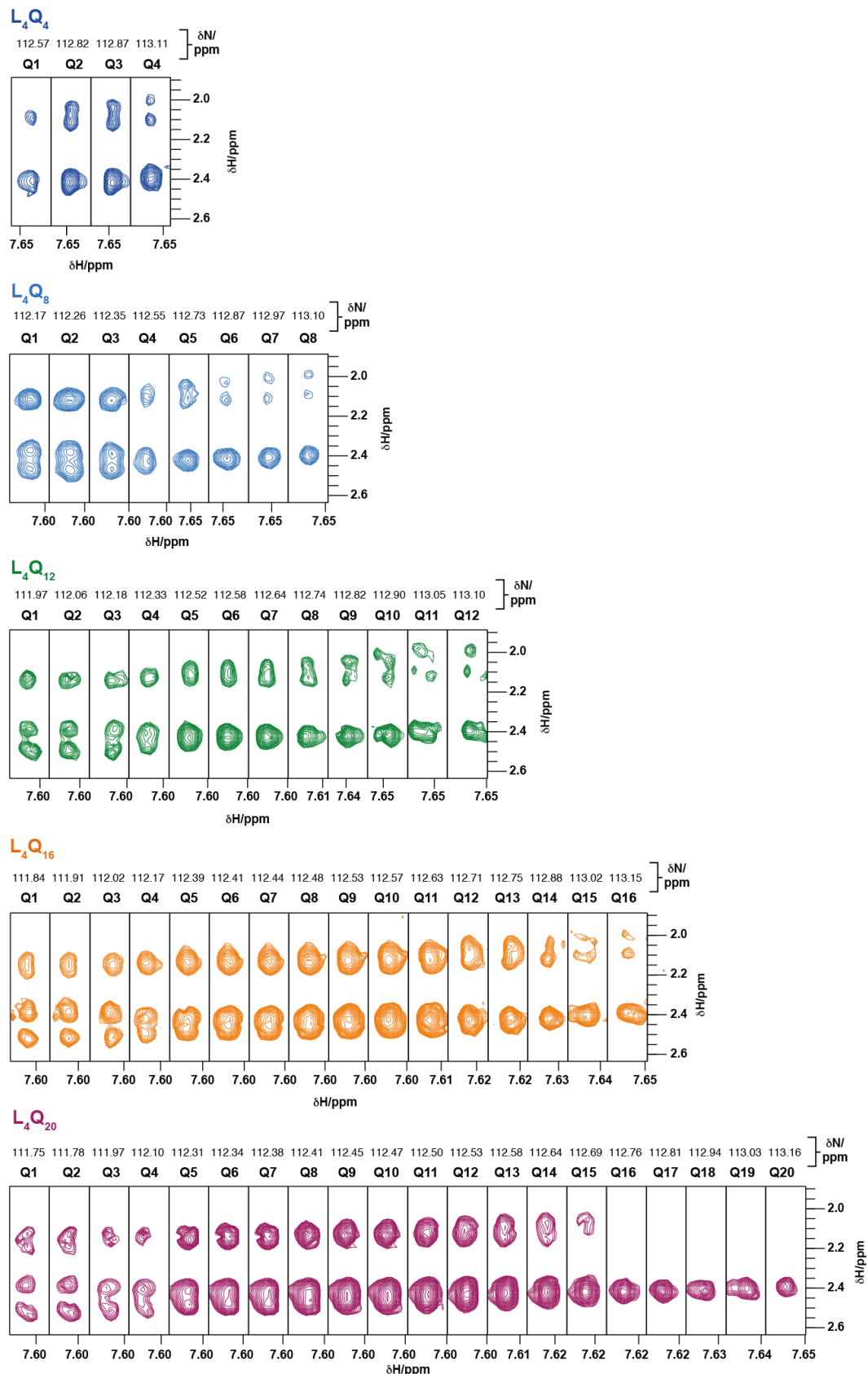
Supplementary Figure 3 | Region of the ^1H , ^{15}N HSQC spectrum of peptides L_4Q_4 to L_4Q_{20} showing the resonances belonging to the backbone amide groups of Gln residues.



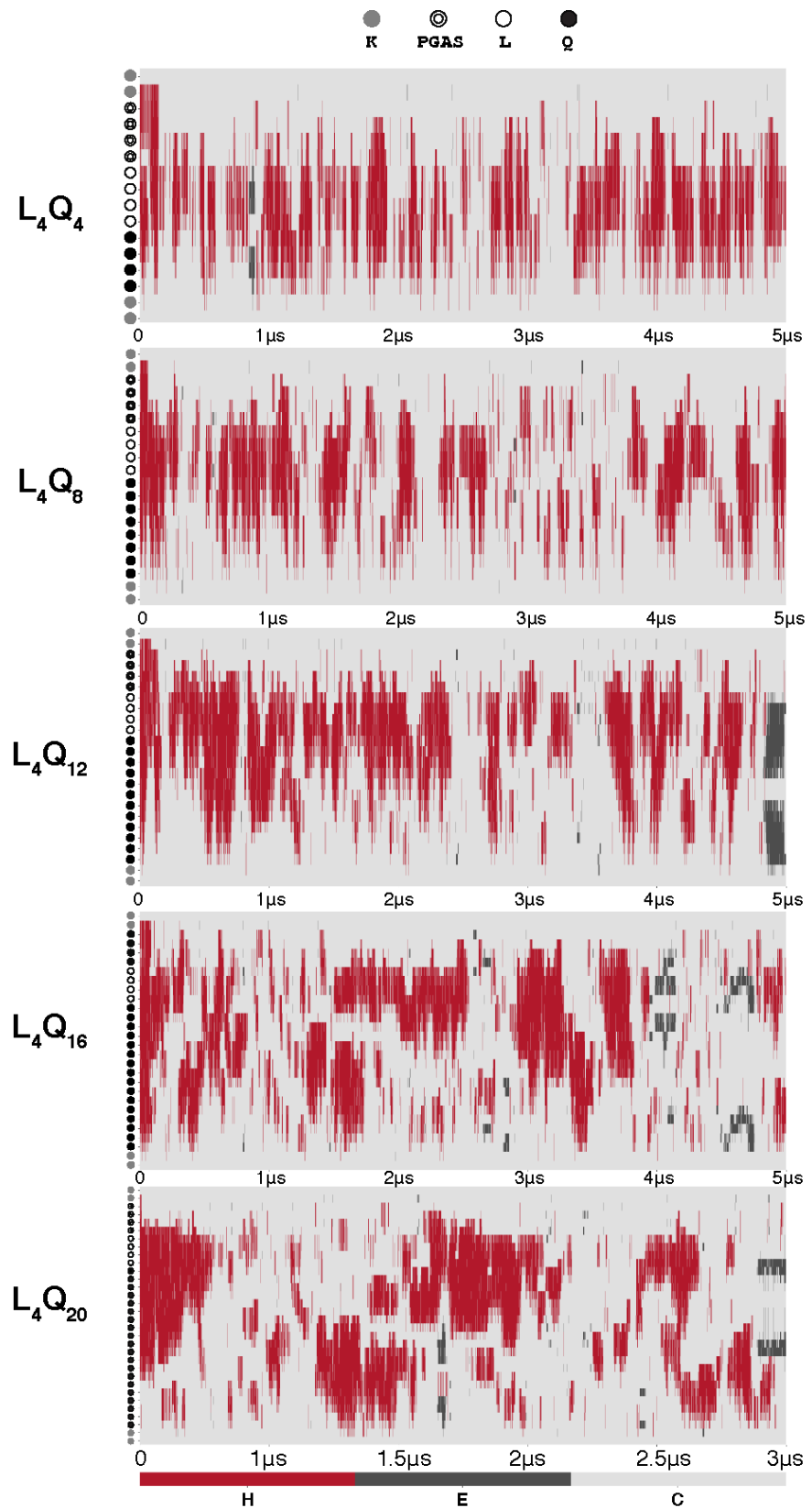
Supplementary Figure 4 | HNCO (light) and HN(CA)CO (dark) spectra of peptides L₄Q₄ to L₄Q₁₆ used for the assignment of the backbone resonances.



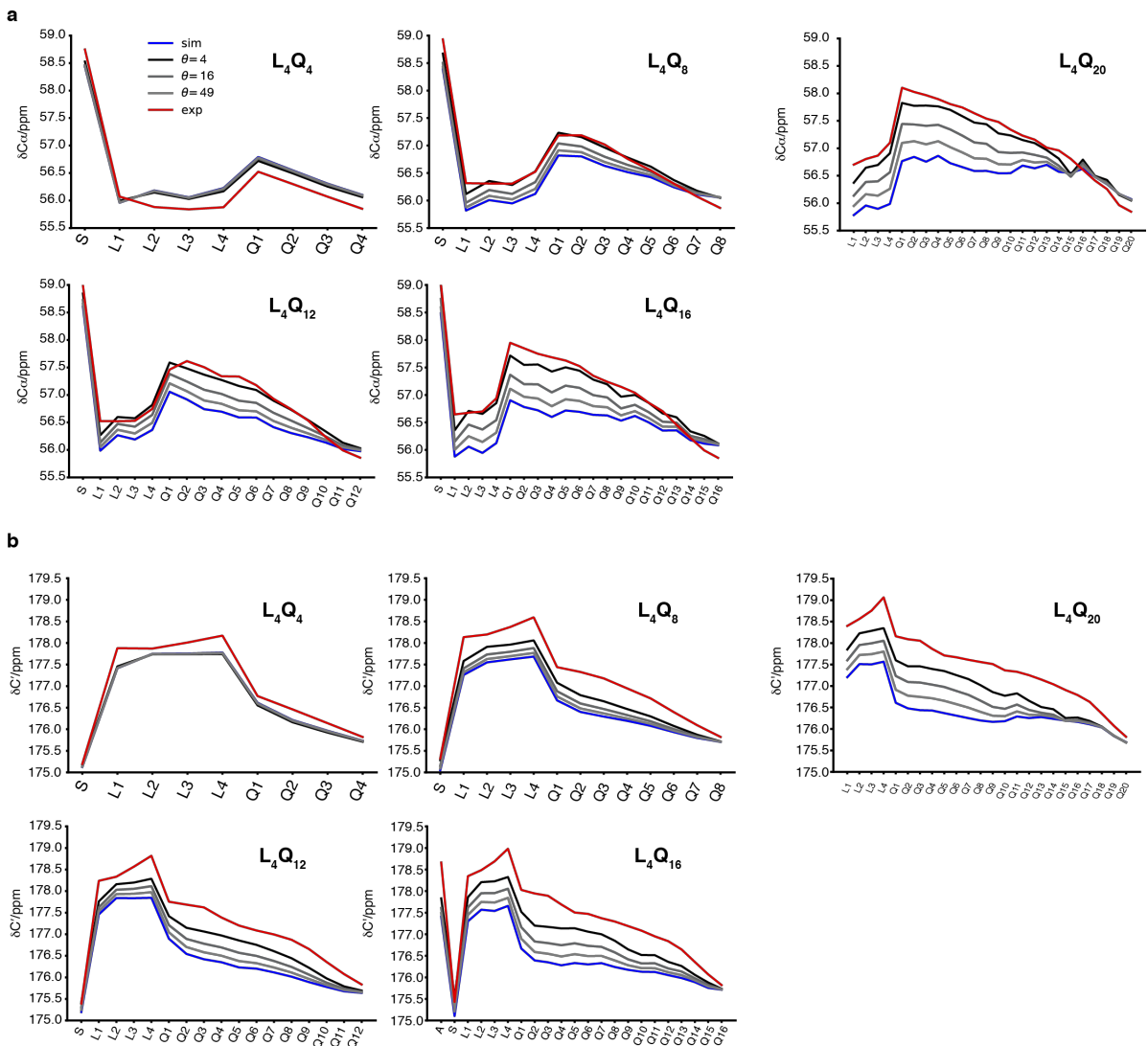
Supplementary Figure 5 | Strip plots showing the Ca cross-peaks correlated to the main chain NH resonances in the $\text{HN}(\text{CO})\text{CACB}$ experiment (light) and side chain $\text{NH}\epsilon_{21}$ resonances in the $(\text{H})\text{CC}(\text{CO})\text{NH}$ experiment (dark), used in the assignment of the latter.



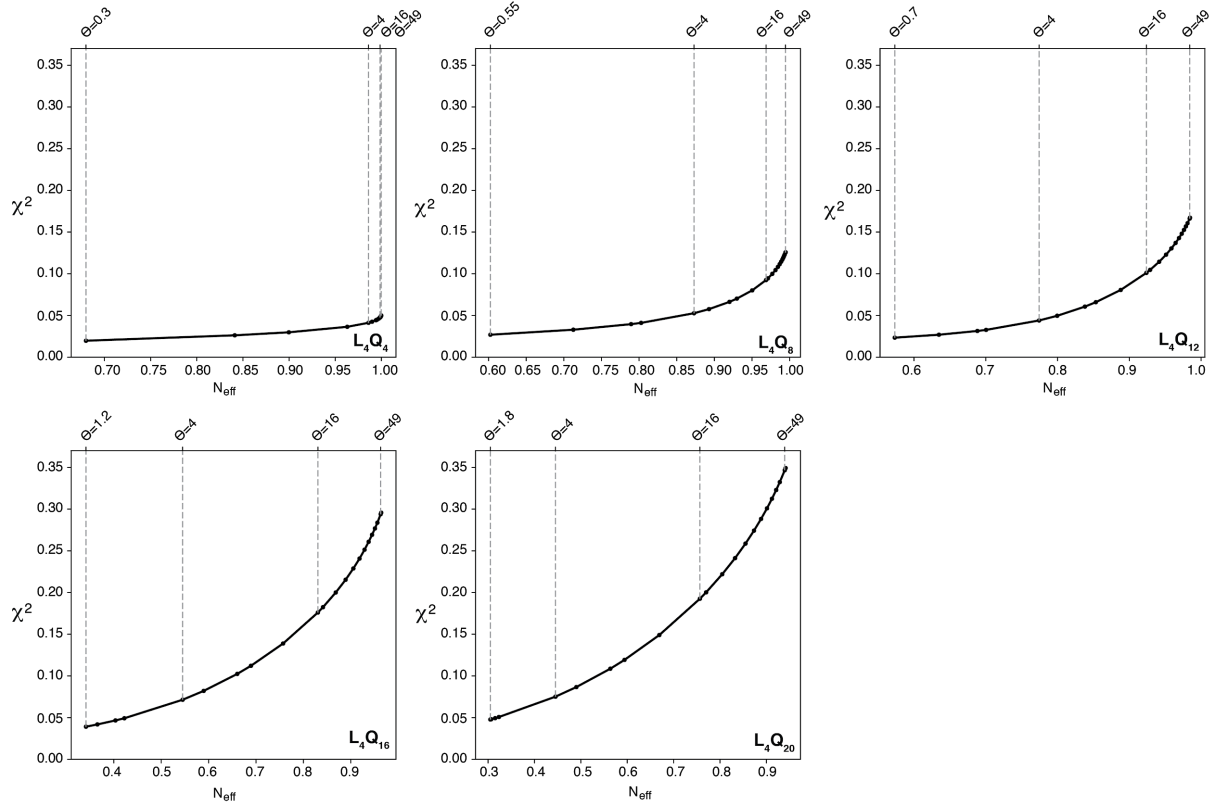
Supplementary Figure 6 | Hε₂₁-centered regions of the ¹⁵N planes of the H(CC)(CO)NH spectra of peptides L₄Q₄ to L₄Q₂₀ containing the side chain aliphatic ¹H resonances of all residues of the polyQ tract.



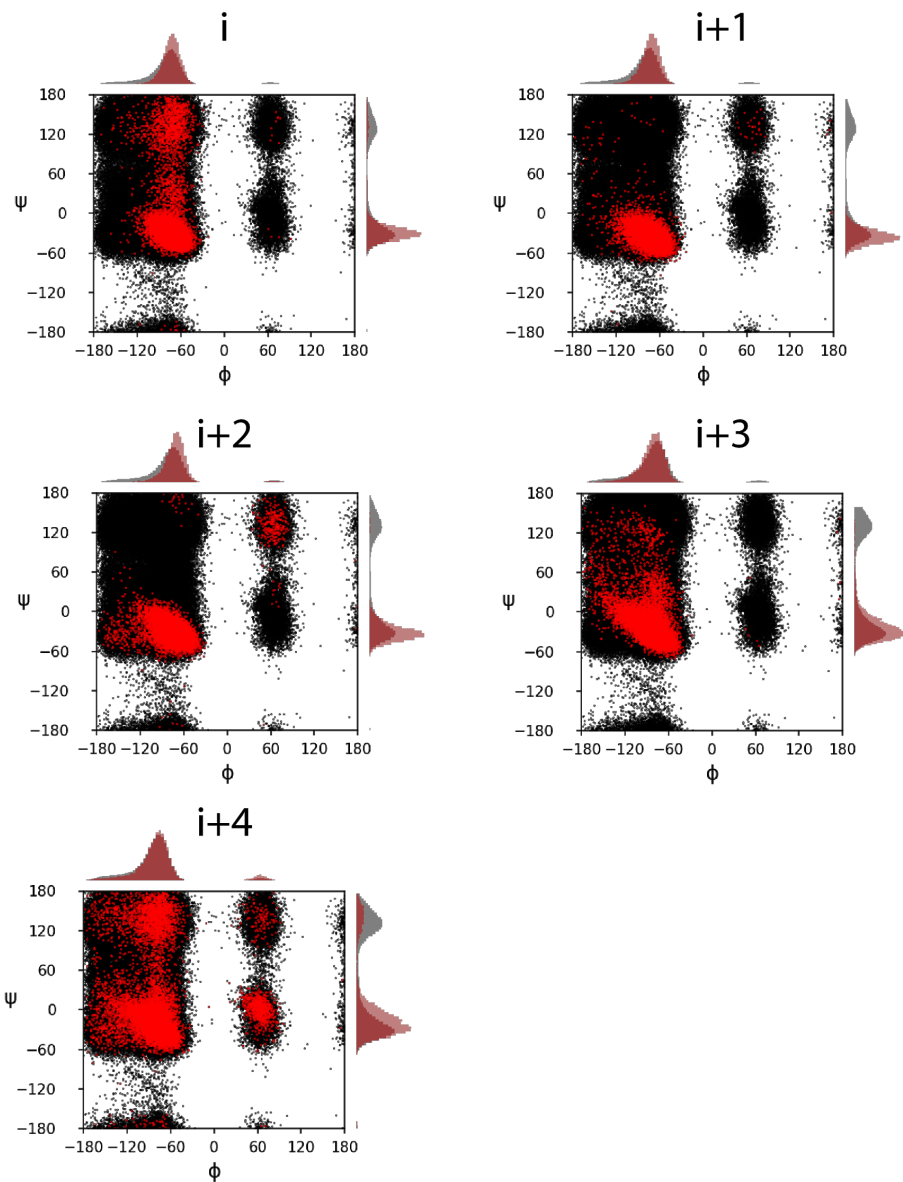
Supplementary Figure 7 | Time series of the secondary structure of peptides L_4Q_4 to L_4Q_{20} as obtained by using the algorithm DSSP² where H stands for helix, in red; E stands for extended, in dark gray; and C stands for coil, in light gray.



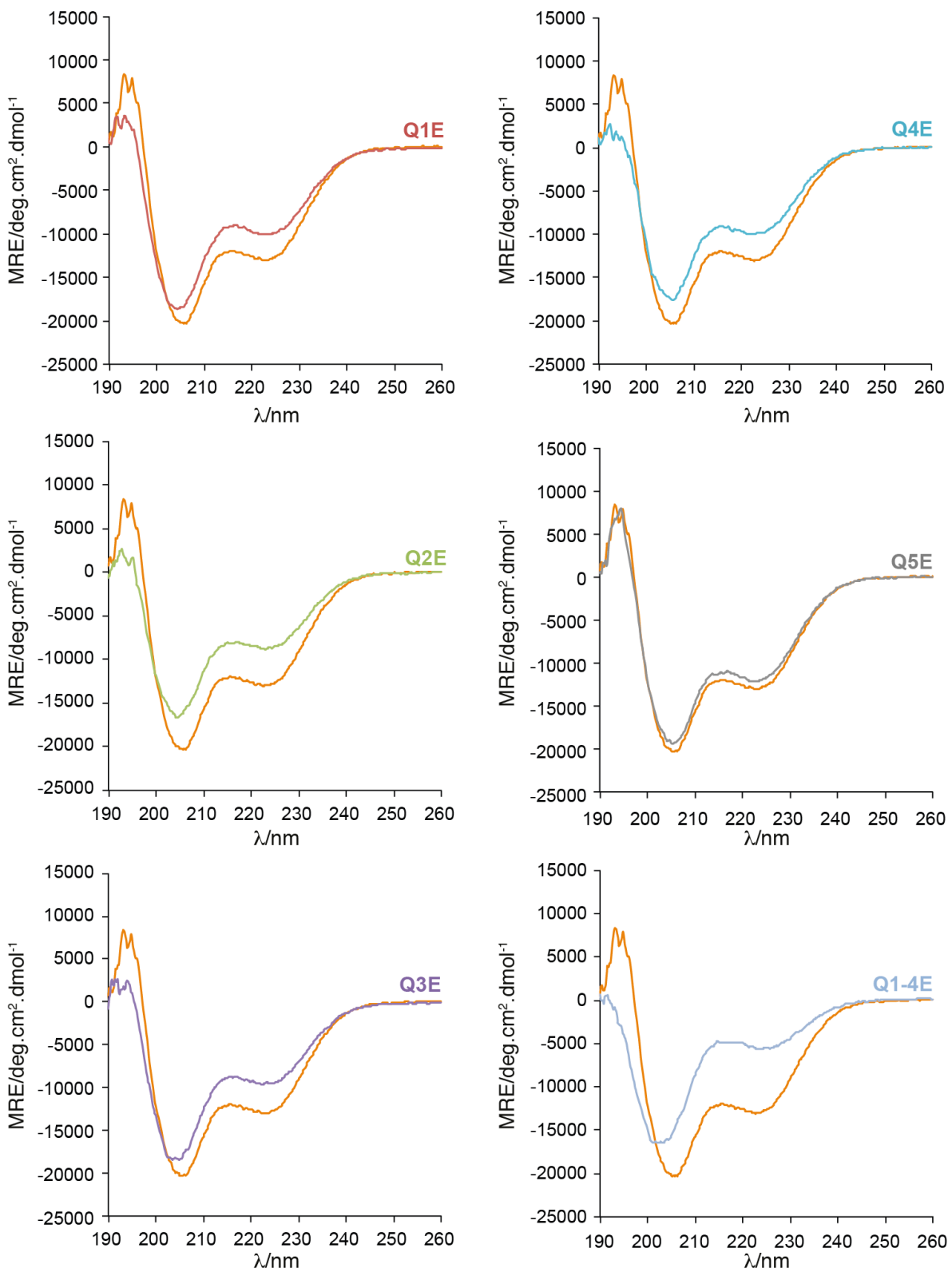
Supplementary Figure 8 | Experimental and back-calculated (a) C α and (b) C' chemical shifts of peptides L₄Q₄ to L₄Q₂₀ from the reweighted trajectories obtained with different values of the parameter θ , that determines the degree of reweighting applied in the ME algorithm.



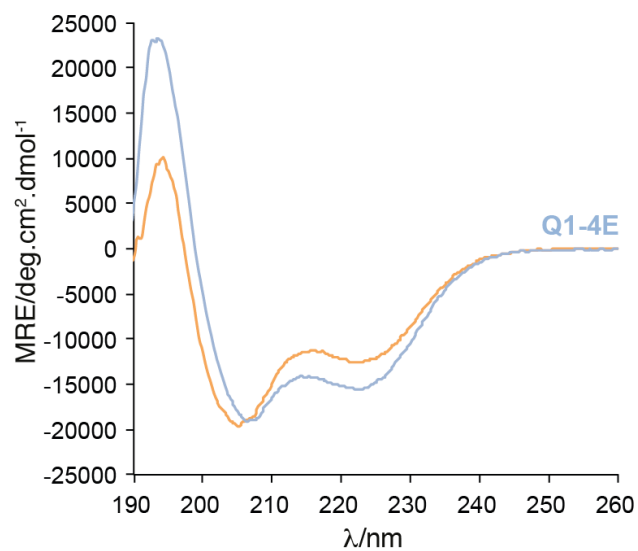
Supplementary Figure 9 | Effective fraction of frames after reweighting vs χ^2 for different values of θ . N_{eff} was calculated as $\exp(S_{\text{rel}})$ with S_{rel} being the relative entropy term in the BME reweighting approach. In short, N_{eff} quantifies the effective fraction of frames that are left after the trajectory has been reweighted to fit the data to an extent measured by χ^2 .



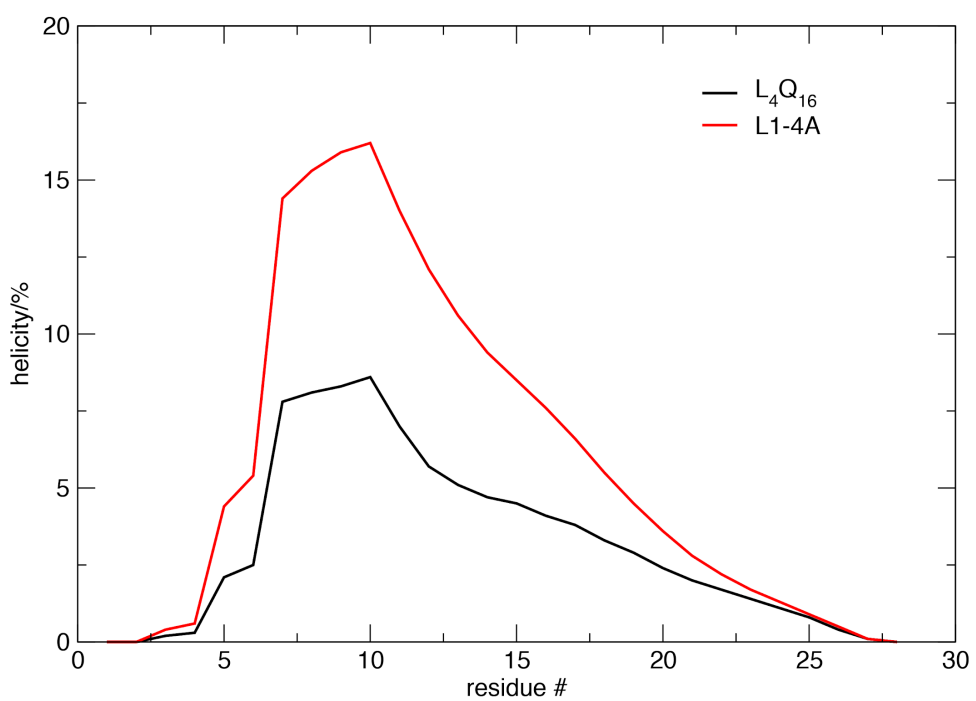
Supplementary Figure 10 | 2D histogram, in red, of backbone torsion angles ϕ and ψ for segments of five residues where the first and last residue are involved in a $(i+4 \rightarrow i)$ side chain to main chain hydrogen bond. In black we show the result obtained when these residues are not involved in such interaction.



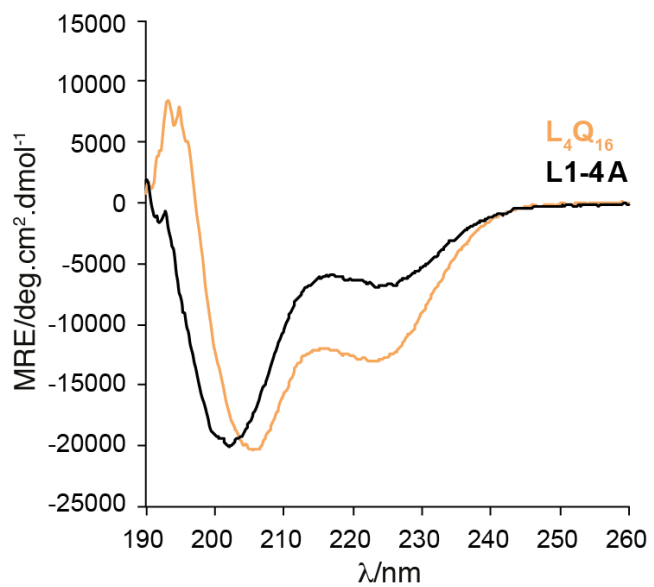
Supplementary Figure 11 | Comparison of the CD spectra of peptides Q1E to Q5E, as well as that of peptide Q1-4E, to that of peptide L₄Q₁₆, shown in orange in all plots.



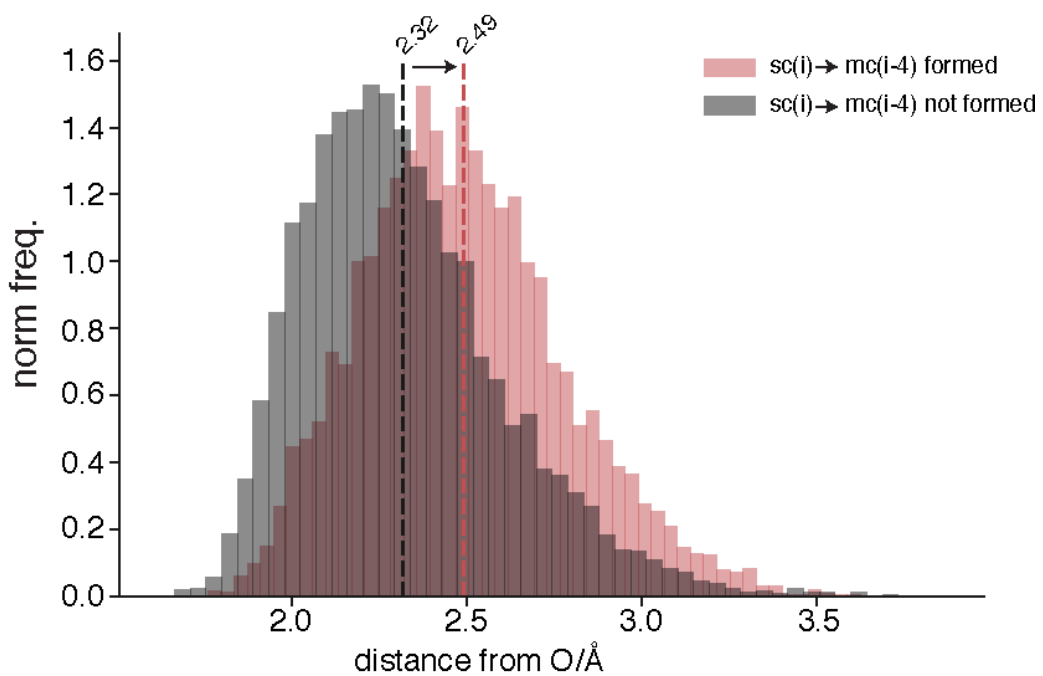
Supplementary Figure 12 | CD spectra of peptides L_4Q_{16} (in orange) and Q1-4E at pH 2



Supplementary Figure 13 | Prediction of the helicities of peptides L_4Q_{16} and L1-4A obtained by using Agadir¹.



Supplementary Figure 14 | Comparison of the CD spectrum of peptide L1-4A, to that of peptide L₄Q₁₆.



Supplementary Figure 15 | Distribution of the distance between the main chain NH of Q1 and the main chain CO of L1 in the absence and in the presence of the $\text{sc}(\text{Q1}) \rightarrow \text{mc}(\text{L1})$ hydrogen bond.

L₄Q₄

ATGAGCGATAGCGAAGTTAATCAAGAAGCCAAACCGGAAGTTAACGCCGGAAAGTGAAACCTG
AAACACATATTAACCTGAAAGTGAATGGCAGCAGCGAAATCTTCTCAAAATCAAAAAA
ACCACACCGCTCGTCGTCGATGGAAGCATTGCAAAACGTCAGGGTAAGAAAATGGATA
GCCTGCCTTCTGTATGATGGTATTCTGAGCAGATCAGACACCCGAAGATCTGGAT
ATGGAAGATAACGATATTATCGAACATCGTGAGCAGATTGGTGGTAAAAAACCGGGTG
CAAGCCTGCTGTTACTGCAGCAGCAACAGAAAAATGATAA

L₄Q₈

ATGAGCGATAGCGAAGTTAATCAAGAAGCCAAACCGGAAGTTAACGCCGGAAAGTGAAACCTG
AAACACATATTAACCTGAAAGTGAATGGCAGCAGCGAAATCTTCTCAAAATCAAAAAA
ACCACACCGCTCGTCGTCGATGGAAGCATTGCAAAACGTCAGGGTAAGAAAATGGATA
GCCTGCCTTCTGTATGATGGTATTCTGAGCAGATCAGACACCCGAAGATCTGGAT
ATGGAAGATAACGATATTATCGAACATCGTGAGCAGATTGGTGGTAAAAAACCGGGTG
CAAGCCTGCTGCTCAGCAGCAACACAGCAACAGCAACACAGCAGAAGAAGTG
ATAA

L₄Q₁₂

ATGAGCGATAGCGAAGTTAATCAAGAAGCCAAACCGGAAGTTAACGCCGGAAAGTGAAACCTG
AAACACATATTAACCTGAAAGTGAATGGCAGCAGCGAAATCTTCTCAAAATCAAAAAA
ACCACACCGCTCGTCGTCGATGGAAGCATTGCAAAACGTCAGGGTAAGAAAATGGATA
GCCTGCCTTCTGTATGATGGTATTCTGAGCAGATCAGACACCCGAAGATCTGGAT
ATGGAAGATAACGATATTATCGAACATCGTGAGCAGATTGGTGGTAAAAAACCGGGTG
CAAGCCTGCTGCTCAGCAGCAACACAGCAACAGCAACACAGCAGAAGAAGTG
ATAA

L₄Q₁₆

ATGAGCGATAGCGAAGTTAATCAAGAAGCCAAACCGGAAGTTAACGCCGGAAAGTGAAACCTG
AAACACATATTAACCTGAAAGTGAATGGCAGCAGCGAAATCTTCTCAAAATCAAAAAA
ACCACACCGCTCGTCGTCGATGGAAGCATTGCAAAACGTCAGGGTAAGAAAATGGATA
GCCTGCCTTCTGTATGATGGTATTCTGAGCAGATCAGACACCCGAAGATCTGGAT
ATGGAAGATAACGATATTATCGAACATCGTGAGCAGATTGGTGGTAAAAAACCGGGTG
CAAGCCTGCTGCTCAGCAGCAACACAGCAACAGCAACACAGCAGCAACACA
ACAGAAAAAGTAATAA

L₄Q₂₀

ATGAGCGATAGCGAAGTTAATCAAGAAGCCAAACCGGAAGTTAACGCCGGAAAGTGAAACCTG
AAACACATATTAACCTGAAAGTGAATGGCAGCAGCGAAATCTTCTCAAAATCAAAAAA
ACCACACCGCTCGTCGTCGATGGAAGCATTGCAAAACGTCAGGGTAAGAAAATGGATA
GCCTGCCTTCTGTATGATGGTATTCTGAGCAGATCAGACACCCGAAGATCTGGAT
ATGGAAGATAACGATATTATCGAACATCGTGAGCAGATTGGTGGTAAAAAACCGGGTG
CAAGCCTGCTGCTCAGCAGCAACACAGCAACAGCAACACAGCAGCAACACA
ACAACAGCAGCAACAGAAGAAAATGATAA

Supplementary Table 1 | Codon-optimized sequences used for the expression of peptides L₄Q₄ to L₄Q₂₀

Supplementary References

1. Muñoz, V. & Serrano, L. Elucidating the folding problem of helical peptides using empirical parameters. *Nat. Struct. Biol.* **1**, 399–409 (1994).
2. Kabsch, W. & Sander, C. Dictionary of protein secondary structure: pattern recognition of hydrogen-bonded and geometrical features. *Biopolymers* **22**, 2577–2637 (1983).